

Quantifying the performance of high-throughput directed evolution protocols

Adèle Dramé-Maigné*, Anton Zadorin*,
Iaroslava Golovkova, Yannick Rondelez

Laboratoire Gulliver, CNRS, ESPCI Paris, PSL Research University, 10 rue Vauquelin, Paris, France. * equally contributed to this work.

Abstract

Most protocols for the high-throughput directed evolution of enzymes rely on random encapsulation to link phenotype and genotype. In order to optimize these approaches, or compare one to another, one needs a measure of their performance at extracting the best variants. We introduce here a new metric named the Selection Quality Index (SQI), which can be computed from a simple mock experiment with a known initial fraction of active variants. As opposed to previous approaches, our index integrates the random co-encapsulation of entities in compartments and comes with a straightforward experimental interpretation. We further show how this new metric can be used to extract general trends of protocol efficiency, or reveal hidden mechanisms such as a counterintuitive form of beneficial poisoning in the Compartmentalized Self-Replication protocol.

Introduction

Molecular Directed Evolution (DE) is a technique to obtain biomolecules with desirable or improved functions, by iteratively generating pools of randomized variants and screening or selecting them to extract the best performers from these pools. This technique, initially developed for the search of nucleic acid ligands[22, 12], has been extended to proteins and used to explore other chemistries and functions [6, 2]. Most importantly, it is now also used to select biopolymers with tailored catalytic properties, i.e. artificial enzymes[3].

The first high-throughput enzymes DE experiments used living cells as a selection medium for the mutant phenotypes. In such *complementation* approaches, the cell expression machinery is employed to translate an exogenous randomized genetic element into the corresponding mutated polypeptide. Additionally, survival and replication of the host cells is made dependent on the

catalytic activity provided by the exogenous gene. Selection between desirable and undesirable phenotypes becomes possible for two reasons: first, the cell boundaries ensure that the genotype-phenotype linkage is maintained, and that selection, acting on phenotypes, yields improved transferable genotypes; second, cell transformation strategies provide a straightforward way to obtain populations of cells where each member contain one and only one of the possible mutant genotypes. Alternatively, when no strong coupling between the exogenous phenotype and host cell survival can be achieved, screening methods, where the cells can be sorted according to an observable marker of phenotype, have been designed.

While these *in vivo* implementations are very efficient, they still suffer from a number of technical issues. First, complementation approaches are only possible for catalytic activities that are related to the host cell's essential processes. In the screening protocols, permeability of the cell walls to metabolite may interfere with the diffusion of substrate to the catalyst. Finally, in both cases, the strategy has to be compatible with the metabolic function of the living host; activities that are toxic for the host gets naturally counter-selected, in some case disrupting the intended DE process.

To bypass these problems, a number of recent developments have introduced the idea of performing high-throughput directed enzyme evolution *in vitro*[14, 11, 15, 4, 18, 7, 23, 20, 1, 5, 13]. In these protocols, mutant genotype-phenotypes are randomly distributed in artificial micro-compartments, with an internal volume ranging between the femtoliter and the nanoliter. As is the case for DE using living organisms carriers, two strategies can be used to extract the best genotypes: screening and selection. In screenings, the phenotypes induce a detectable modification of the physico-chemistry of the compartment, which is used to sort the compartments one-by-one into desirable and non-desirable bins[4]. In selection approaches, the artificial compartment additionally enables a biochemical genetic amplification process, directed at the gene of interest and whose activation is conditional on the desired activity.

A common important feature of these high-throughput *in vitro* protocols is that they use a *random* distribution of the mutant library in the artificial micro-compartments (usually droplets, but also liposomes, micro-patterned arrays[21], etc). By contrast with the case of *in vivo* approaches, *in vitro* protocols provide no internal mechanism to insure that one and only one genotype will be present in each compartment. As a consequence, one can only control the *average* number of mutants per compartment (a value referred as λ in the following discussion) but not their actual repartition in the compartment population. If the partitioning process is truly random, the distribution of occupancy will follow the Poisson law. For example, if λ is set to 1 (i.e. there are as many compartments as mutants genotypes), the proportion of compartment containing 0, 1 and more than one genotypes will be roughly one third each. Lowering the values of λ yields more wasted (unoccupied) compartments, while higher values increases the number of compartments containing multiple genotypes.

High-throughput protocols are therefore fundamentally stochastic, and their purpose is to increase the proportion of highly functional variants after each

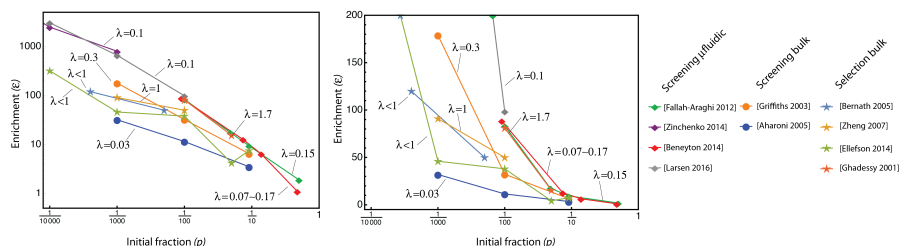


Figure 1: Reported enrichment factors from a selection of references. The enrichment factor is plotted in linear (right) or log (left) scale against the initial fraction of active mutants used in the experiment. Lines connect data points from the same manuscript, and obtained with a single value of λ (indicated next to the line). Disks are used for protocol using screening and polydisperse emulsions; diamonds, for protocols using screening and monodisperse (microfluidic) emulsions; Stars, for protocols using selections in polydisperse emulsion. Some values were recomputed from the reported data. See SI for details.

round. Their performance at enriching libraries will depend on a number of experimental choices or constraints. These factors include the value of λ , but also, for example, the contamination by parental genotype, the homogeneity of the compartment’s physicochemical parameters, or the robustness of the genotype-phenotype linkage, etc. Various experimental approaches have been proposed, with different throughput and performance. Assessing the relative efficiency of the methods and the particular contribution of these factors on a given DE protocol can be challenging.

Enrichment factor

In an attempt to characterize the quality of a given high-throughput directed evolution protocols, many papers report a so-called enrichment factor $\varepsilon = \frac{p'}{1-p'} \cdot \frac{1-p}{p}$, where p and p' are the frequencies of the allele of interest before and after one selection cycle, respectively (in some cases the enrichment factor is defined using the simple ratio of frequencies, $\varepsilon = p'/p$). To evaluate the value of this enrichment factor for a given protocol, an experiment is set up where the initial library contains a small proportion of active variants among many inactive ones, and this proportion is measured again after a single selection round. Generally, to perform these experiments, a mock library containing only two versions of the target protein, an active and an inactive one, is used. A compilation of reported values of ε from various reports is given in Fig 1, while the full tables are included in SI Material & Methods (Table S2, S3, S4).

However, the usage of ε as a measure of quality comes with a number of issues:

- First, ε depends strongly both on the initial fraction of functional mutants

p and on the value of λ . As can be seen in Fig 1, measurements of enrichment factors made with different values of p generally yield values of ε that vary over many orders of magnitude. Similarly, changes in λ yield different enrichment factors, with no clear interpretation.

- Second, the upper theoretical limit of ε is infinity when p or λ become small. This reflects the fact that in principle, a flawless selection or screening assay should get rid of the poor phenotype in a single round. It is therefore difficult to estimate what should be a correct, or acceptable, value of an experimental ε . In practice, smaller values of p or λ tend to increase the observed value of ε , suggesting, against common knowledge, that the protocol performs better on less rich libraries. Additionally, measurements at very small λ are not really useful in assessing a protocol meant to provide the highest possible throughput, as the throughput is actually proportional to λ . Note that the theoretical lower limit of ε is 0 at high p or high λ . Every value below 1 would indicate a process that counter-selects for the good genotype.

Altogether, interpreting the enrichment factor is difficult and it is clear that one cannot use it directly to compare different protocols in terms of their ability to enrich libraries. We introduce here an improved performance metrics, the Selection Quality Index (SQI). The SQI is expressed as a fraction of the theoretical (achievable) value for the selection of a functional variant from a pool of lethal variants and normalizes for the effect of p and λ . An SQI of 1 denotes a perfect protocol, whereas an SQI of 0 indicates a complete failure, i.e. the absence of any enrichment effect (negative values indicate counter-selection). Accordingly, this index -in combination with the throughput of the protocol- can be used to assess the true absolute potential of a given experimental approach to concentrate rare catalytic variants. It can also be used to compare different protocols, or different variants of the same protocol.

Model

The factors that control the change in frequency of a mixture of active and inactive mutants in a high-throughput protocol can be separated in two groups.

The first group contains controllable or known parameters of the experimental design: λ , the sharing status, and the replication/selection function. These effects are detailed below:

- As mentioned above, when λ increases, a fair fraction of the compartments actually contain more than one phenotype, leading to the possibility of “hitch-hiking”. Inactive mutants, which should not have survived the screening or selection process, are carried over by sharing a compartment with a better phenotype. In principle, knowledge of the compartmentalization process allows us to describe the distribution of occupancies. For example, in the case of random compartmentalization, this distribution will follow a Poisson law.

- The second effect, also linked to the random co-encapsulation of variants, is fitness sharing. This occurs when the presence of the poor phenotype is actually detrimental to the good one. This is typically the case in selection experiments: an equal fraction of the replication potential associated with one compartment will be used to amplify each local variant, whether or not they actually contributed to the replication activity. This sharing effect does not happen in screening protocols, which works by discarding the low activity compartments, rather than replicating the genotypes in the good ones. In other words, in screenings, a variant present in a supra-threshold compartment contributes one genotype to the next generation irrespective of the presence of co-encapsulated variants in his compartment. These two situations are referred as sharing and non-sharing, respectively, in the rest of the manuscript.
- Third, the replication/selection function [25], which describes how many genotypic copies are pushed to the next generation, according to the phenotypic activity observed in a compartment. In screenings for example, the value of the function is one if the phenotypic activity is above a given threshold, and 0 otherwise. In selections, it is set by the internal replication chemistry.

The second group consists of experimental idiosyncrasies that are not directly controllable. Together, they explain the observed deviation from a perfect assay. These factors can be based on a variety of causes, some known or guessable, other altogether unknown. For example, in screening test, the sorting machinery may not be 100% efficient or generally makes a number of errors (typically increasing when sorting is attempted at higher frequencies [4]). Noise in expression can also play a role when compartments containing the same genotype may end up with various level of phenotypic activity (typical when bacterial expression systems is used, i.e. lysate assays [18]). Additionally, leaks between compartments, poor genotype-to-phenotype linkage (e.g. in mRNA display strategies), hidden selection biases (e.g. linked to toxicity effect), non-homogeneity or polydispersity of the encapsulating compartments (see below), carry-over of the parent genomes in selections, and a myriad of other causes may affect the result. One typically does not have enough information to precisely describe or model these effects, and is rather interested in quantifying their collective negative impact on the selection protocol, in order to empirically try to minimize it.

The Selection Quality Index (SQI)

We have recently shown that all effects belonging to the first group can be modeled using the single equation (1). This equation describes the evolution of a population of variants submitted to random-compartmentalized selection rounds, characterized by an additive replication/selection function f , a sharing rule $\varphi(n)$ (the fraction of the value given by f allocated as copies to each individual in the droplet of size n), and a distribution of phenotypes ρ ([24]).

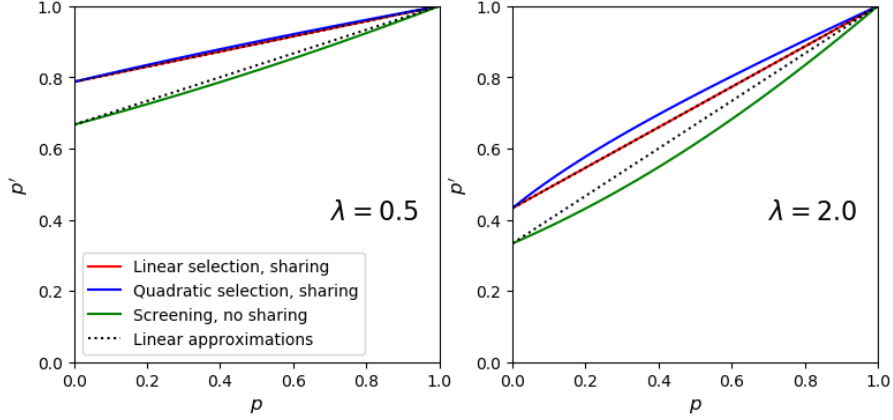


Figure 2: Graphical representation of the expected new fraction p' as a function of initial fraction p for various replication/selection function f and for two values of λ . The exact analytical results derived from (1) are shown by solid lines. The linear approximation is shown by a dotted line for the cases both with and without sharing. Δ corresponds to the intercept of the curves with the vertical axis and is independent of f .

$$\rho' = \frac{\sum_{n=0}^{\infty} \frac{\lambda^n}{n!} \varphi(n+1) \langle \delta_x * \rho^{*n}, f \rangle}{\sum_{n=0}^{\infty} \frac{\lambda^n}{n!} \varphi(n+1) \langle \rho^{*n+1}, f \rangle} \rho \quad (1)$$

where $*$ means convolution of distributions, δ_x is the delta-function centered at x , and $\langle \rho, f \rangle$ means application of the distribution ρ to the function f .

Here, we are interested in quantifying the quality of a typically mock selection protocol where only two variants are used. One of them is active and the second completely dysfunctional (i.e., in isolation, it should not survive the selection process). Therefore ρ has only two discrete values. Equation 1 allows us to compute the theoretical (expected) value of p' as a function of p for different λ , which we will call $p'_{theo}(p)$ (Fig. 2). Importantly, this function is discontinuous at $p = 0$, reflecting the effortless invasion of the population of dysfunctional mutants by a rare functional one. In an ideal selection with no co-encapsulation, the jump observed at low p , corresponding to the selection of one active variant among an infinity of inactive ones would be equal to 1. Therefore, the value of this jump, Δ , provides a good absolute characterization of the selection efficiency at low p , and depends only on λ . Indeed, one can show that the general equation(1) yields an expression for Δ , which does not depend on the replication function f :

$$\Delta = p'_{theo}(p \rightarrow 0) = \frac{\sum_{n=0}^{\infty} \frac{\lambda^n}{n!} \varphi(n+1)}{\sum_{n=0}^{\infty} \frac{\lambda^n}{n!} (n+1) \varphi(n+1)}.$$

However, it is generally not practical to perform experiments at very small p , so we will also need the behavior of p' at $p \rightarrow 0$. As this behavior does depend on f , we propose to correct using a linear approximation of the following form.

$$p'_{theo}(p) \simeq \Delta + (1 - \Delta)p. \quad (2)$$

This expression is exact for linear replication functions and performs well for nonlinear ones (especially, for not very large λ , see Fig. 2). Altogether, we find that all possible scenario collapses into only two cases:

In the non-sharing situation, which is typical of screening protocols, we have $\varphi(n) = 1$ and the theoretical value of Δ as a function of λ is given by:

$$\Delta = \frac{1}{1 + \lambda}. \quad (3)$$

In the sharing situation, which is more typical of selections assay, there is a cost associated with the presence of co-encapsulated variants and $\varphi(n) = 1/n$. We obtain:

$$\Delta = \frac{1 - e^{-\lambda}}{\lambda}. \quad (4)$$

We conclude that, knowing λ and p , and the sharing behavior of a given experiment setup, one can obtain a good approximation of the theoretically expected gene frequency $p'_{theo}(p)$ after one round of selection of a very rare functional mutant in a population of dysfunctional ones. This p'_{theo} can be used as a reference to assess the quality of the experimental protocol, independently of the controllable parameters λ and p . In principle, one can thus use any convenient value of λ and p and simply measure the experimental frequency p'_{exp} after the selection cycle. The SQI of the protocol can then be expressed as the ratio of the experimental to theoretical frequency jumps, i.e:

$$SQI = (p'_{exp} - p)/(p'_{theo} - p). \quad (5)$$

Finally,

$$SQI_{screen} = \frac{(1 + \lambda)(p' - p)}{1 - p} \quad \text{and} \quad SQI_{selection} = \frac{\lambda e^\lambda (p' - p)}{(e^\lambda - 1)(1 - p)}.$$

These formula provide an absolute measurement of protocol quality and selection efficiency, that corrects for p , λ and the sharing behavior. It is independent of the replication/selection function f , and reflects only the experimental contingencies belonging to group 2.

General trends for SQI values

In Fig. 3 we use the reported data shown in Fig. 1 to compute the SQI of a variety of experimental protocols and conditions. This immediately reveals some interesting trends.

First, some of the data series, taken at various but relatively high initial fractions (e.g. for $p \geq 1/100$) collapse to a single SQI value. For example the points from [Fallah-Araghi 2012] and [Beneyton 2014], now give roughly the same SQI, independent of the initial fraction. Additionally, for these relatively high initial fractions, we note a cluster of data points that achieve an SQI close to one, indicating that the best achievable enrichment performance has been attained.

Second, for the lower p values, the selection efficiency always decrease with decreasing initial fractions of active mutants. This stands in striking contrast with the trend observed in Fig. 1, where enrichment factors seemed to indicate that all assays performed much better at lower initial fraction. This apparent trend was just a mechanical consequence of the fact that it is easier to invade a population of dysfunctional mutants, rather than a population already containing a significant fraction of functional mutants. Our analysis corrects for that effect. It thus highlights the fact that other experimental contingencies actually dominate at low p , making experimental protocols less and less ideal as the initial fraction decreases. This is due to a decreasing signal-to-background ratio, where the background noise can result from a variety of effects, such as contamination by parent DNA in selections, sorting errors in screenings, or the difficulty to recover very small amounts of genetic material in the general case.

Third, protocols can be separated according to their type: only screening using microfluidic compartmentalization appear to yield efficiencies close to 1. In contrast, protocols using screening of bulk emulsions typically have a lower performance. This indicates that the size-dispersity of the compartments is an important factor contributing to the efficiency of screenings. In contrast, some selection processes are able to obtain high index without resorting to monodisperse emulsion, which could be related to the superior robustness of selections versus screenings, with respect to co-encapsulation (already noted in [25]). Indeed, reports concerning selections tend to use higher λ values.

Besides these general cross-studies trends, one can also use the SQI to analyze individual experimental setups. For example, In 2009, Baret and colleagues tested the Fluorescent Activated Droplet Sorting method [4] with different conditions, and concluded that poisoning co-encapsulation explained the lower efficiency at higher λ . Re-analysis of these results shows that the SQI, although correcting for λ , decreases clearly as well. This suggests that another cause linked to the increased concentration of cells, e.g. leaks, could explain the behavior.

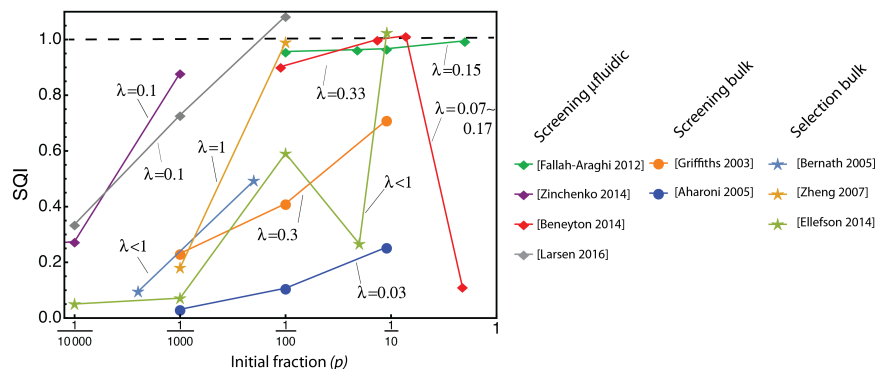


Figure 3: SQI calculated for the data in Fig 1. Lines connect data point originating from the same manuscript, and done with a single value of λ (indicated next to the line). Disks are used for protocol using screening and bulk (non-monodisperse) emulsions; diamonds, for protocols using screening and microfluidic (monodisperse) emulsion; Stars, for protocols using selections in bulk emulsion. The dotted line at = 1 represents the theoretical maximum performance, once initial fraction and random partitioning have been taken into account. Note that the CSR experiment[14] is off scale here (see Fig4).

The SQI reveals deviation to Poisson statistics

The SQI seems to be able to stratify experimental platforms in terms of both the quality of the experimental design, and their reaction to increasingly challenging libraries (that is, containing a smaller and smaller fraction of active variants). One approach, however, seems to stand out in terms of its SQI, which is much above 1 when measured for a high value of $\lambda = 1.7$. This approach is an *in vitro* selection process, termed CSR, for Compartmentalized Self-Replication[14]. It targets a bacterial library of variants of the Taq polymerase gene, which is encapsulated in droplet with Taq-specific primers. After lysis at high temperature and PCR thermal cycling, mutants polymerases with higher activity replicate their own genes better than less active ones. When the droplets are broken, the retrieved genetic population is thus enriched in active Taq variants. According to its SQI, CSR apparently selects active mutants better than the theoretical limit due to random coencapsulation (Fig. 4). This could indicate that this particular selection process (and possibly some other) has a build in mechanism that limits the carryover of inactive variants. To investigate this point, and since, the SQI in this case was evaluated from relatively sparse reported information, we decided to re-implement the experiment.

After a number of failed attempts, we were able to reproduce the CSR with some modifications. First, we used Klentaq[19], a lysate-robust polymerase variant, instead of Taq. We found that his enzyme was expressed at sufficient levels in KRX cells (while the initial report used TG1 cells). And finally we used

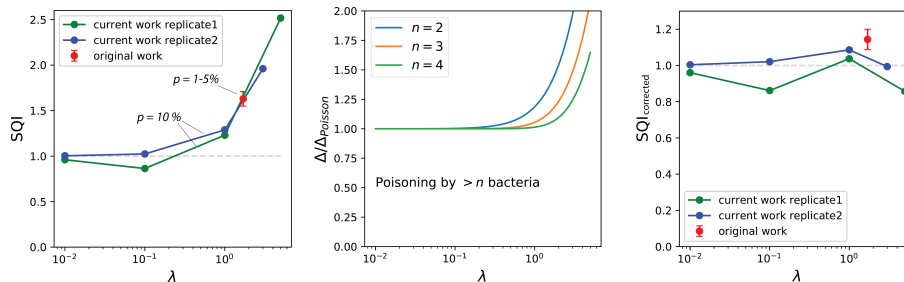


Figure 4: Left: SQR calculated for CSR protocols at various λ . Red: original CSR report[14], in polydisperse emulsion. Blue and green: this work, two independent experimental replicates in monodisperse emulsions. The dotted line at SQR = 1 represents the theoretical maximum efficiency. Middle: Change in expected frequency jump assuming that droplets containing more than n bacteria are poisoned and do not participate in the reaction. Right: The SQR is recomputed with a cutoff set to $n = 2$, corresponding to the experimental observation that PCR is quickly poisoned by excess lysate.

monodisperse droplets in fluorinated oils, instead of the polydisperse emulsion in mineral oil initially reported (see SI experimental section). Given these adjustments, we were indeed able to observe the self-replication of the polymerase gene, both in bulk solution, and in $24 \mu\text{m}$ droplets. We thus measured SQR at different values of λ , as shown in Fig 4. These measurement showed that the CSR process is indeed able to perform optimally at low λ values, where the SQR is roughly 1. It also confirmed that higher λ result in SQR clearly above 1, and therefore that the CSR reaction is somehow immune to random co-encapsulation.

In the course of the experiments, we also noted that the self-PCR reaction performed less efficiently when higher concentration of bacteria were used in the master mix. This is most likely associated with the strong toxicity of the bacterial lysate toward the PCR reaction[17]. We thus reasoned that this phenomenon could explain the observed behavior: if droplets containing more than one bacteria are unable to support PCR, whatever the mixture of active and inactive variants they contain, then they simply do not contribute to the new generation. Therefore, it is as if co-encapsulation would not occur and the jump in frequency should be less affected (Fig. 4 Middle). We therefore performed the reaction, in test tubes, with a mixture of variants that reproduce the content of droplet containing one active, plus increasing amount of inactive variants (see SI experimental section). Indeed, we find that the self-PCR reaction yield decreases a lot as soon as a single inactive variant is encapsulated with an active wild-type. The reaction does not happen with two or more encapsulated inactive bacteria. Fig. 4 right shows the recomputed SQR taking this observation into account. In the case, the corrected SQR stays close to 1 for all experiments, irrespective of the value of λ .

Discussion

In this manuscript, we derive in a rigorous way a metric that can be used to evaluate and compare experimental high-throughput directed evolution protocols. Like previous approaches it requires a mock experiment, where a known mixture of functional and dysfunctional variants is submitted to one selection round, and the change in frequency is evaluated. However, contrary to its predecessors, our metric separates experimental design in two categories, depending on whether they are controllable design parameters or not. We incorporate the value of initial fraction p and the average occupancy λ in the calculation of the score, to provide a metric that is independent on these factors and only reflects other, less controlled causes that may affect the efficiency of a protocol.

When applied to reported data, we observe that the SQI indeed provide an informed evaluation of protocol quality. The fact that it corrects for p and λ allows us to extract trends by comparing different experimental approach and make hypothesis about the cause for the observed differences in efficiency. It also clearly reveals the effect of decreasing signal-to-background values, when the initial fraction of active mutants becomes very small. This approach allowed to detect abnormal selection efficiency, and link this behavior to a deviation from the model of additive fitness, most probably due to the toxicity of bacterial lysate. Counterintuitively, these toxic effects have a positive effect of the selection efficiency.

The equations presented above are valid when individual mutants are *randomly* distributed in the available compartments. In this case, one indeed obtains a poissonian distribution of the number of mutant per compartment, on which we have based our analysis. However, other distributions can be more relevant in some cases. For example, some microfluidic devices use physical effects to encapsulate objects in compartments with distribution sharper than the poisson distribution[16, 8, 9, 10]. Alternatively, mutants candidates can have a tendency to stick or aggregate to each other (for instance in pairs, triples, tetrads, etc.), which will also distort the distribution away from the poisson law. Polyploidy represent a related case, although closer in context to population dynamics than directed evolution protocols. Fortunately, our mathematical approach is general enough to handle many of these cases, and yield theoretical values of Δ in closed analytical form, when available.

The corresponding mathematical derivations are provided in SI. For example, Fig 5 shows the effect of aggregated partitioning in pairs or triplets. When λ is small, we recover the intuitive result that the best possible outcome in terms of frequency jump is the inverse of the aggregation cluster size (i.e., in the case of k -clusters, the good variant can not invade more than $1/k$ of the population in one round). However, the negative effect of aggregation gets offset when λ increases, as all curves gather on the same asymptote, which depends only on the sharing behavior. Interestingly, clustered selection tends to be more resilient to reasonable increases in λ than unclustered selection (Fig 5, left inset).

Many high throughput *in vitro* DE protocols use emulsions as a convenient way to provide compartments. Our bibliographic analysis has also highlighted

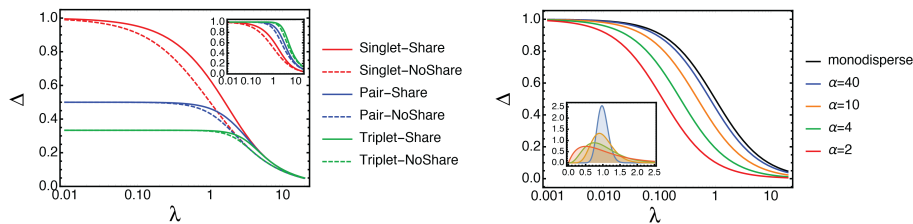


Figure 5: Right, the effect of aggregation of the mutants in pairs or triplets on the theoretical value of Δ (the achievable frequency jump in one round, valid for low p). Full lines correspond to sharing while dotted lines indicate no sharing. Red; encapsulation of discrete individual; Blue, encapsulation in pairs; green, encapsulation in triplets. Inset, the rescaled curves $\Delta/\Delta_{\lambda=0}$. Left, the effect of polydispersity of the compartment in the case of screenings. Here we assume that the volumes are Gamma-distributed with mean one, and various shape parameter α . The corresponding distributions are shown in inset.

the role of the mono/poly-dispersity of these emulsions on the selection process. At equal average compartment volume, polydisperse emulsion will have more compartments containing multiple mutants. This is expected to decrease their efficiency at selecting one particular phenotype from a mixture. Indeed, in the present case of selection from a active/inactive mixture of variants, we can show that the polydisperse emulsion always perform worse than the monodisperse setting. This effect is shown for Gamma-distributed compartment volumes, in the case of screening, in Fig. 5 right.

In conclusion, our analysis suggests that experimentalists using high throughput methods to search for catalysts should put their efforts on improving the efficiency of their protocols at very low initial fractions. Indeed, many protocols target a throughput somewhere between $T = 10^6$ and $T = 10^9$ and it seems unlikely that a very rare active mutant can be purified in a single round. However, at low p , according to the equation 5, the SQI can be written as

$$SQI = p'/p'_{theo}(p) \sim p'/\Delta.$$

This means that knowing λ , and hence Δ , the SQI directly provides an estimation of the final fraction of active mutant (see 2). Many (mostly microfluidic) approaches already provide a good SQI at $p > 10^{-3}$, implying immediate fixation in these cases. It is therefore the ability to bring rare variants (with an initial fraction that can be estimated as the inverse of the throughput of the protocols) to $p' = 10^{-3}$ that is going to be critical for real applications. For example, if an SQI $> 10^{-3}$ is obtained for p as low as $1/T$, then one needs only two rounds to harness the full potential of the experimental protocol, that is, fix a functional variant initially present as a single copy in the library.

Acknowledgements

This work was supported by the ERC Grant “ProFF” (number 647275).

References

- [1] Jeremy J. Agresti, Eugene Antipov, Adam R. Abate, Keunho Ahn, Amy C. Rowat, Jean-Christophe Baret, Manuel Marquez, Alexander M. Klibanov, Andrew D. Griffiths, and David A. Weitz. Ultrahigh-throughput screening in drop-based microfluidics for directed evolution. *Proceedings of the National Academy of Sciences of the United States of America*, 107(9):4004–4009, March 2010. WOS:000275131100014.
- [2] Frances H. Arnold. Directed Evolution: Bringing New Chemistry to Life. *Angewandte Chemie International Edition*, 57(16):4143–4148, April 2018.
- [3] Frances H. Arnold and George Georgiou, editors. *Directed Enzyme Evolution: Screening and Selection Methods*. Humana Press, Totowa, N.J, 2003 edition edition, May 2003.
- [4] Jean-Christophe Baret, Oliver J. Miller, Valerie Taly, Michaël Ryckelynck, Abdeslam El-Harrak, Lucas Frenz, Christian Rick, Michael L. Samuels, J. Brian Hutchison, Jeremy J. Agresti, Darren R. Link, David A. Weitz, and Andrew D. Griffiths. Fluorescence-activated droplet sorting (FADS): efficient microfluidic cell sorting based on enzymatic activity. *Lab on a Chip*, 9(13):1850–1858, July 2009.
- [5] Thomas Beneyton, Faith Coldren, Jean-Christophe Baret, Andrew D. Griffiths, and Valerie Taly. CotA laccase: high-throughput manipulation and analysis of recombinant enzyme libraries expressed in *E. coli* using droplet-based microfluidics. *Analyst*, 139(13):3314–3323, 2014. WOS:000337125600014.
- [6] K Chen and F H Arnold. Tuning the activity of an enzyme for unusual environments: sequential random mutagenesis of subtilisin E for catalysis in dimethylformamide. *Proceedings of the National Academy of Sciences of the United States of America*, 90(12):5618–5622, June 1993.
- [7] Pierre-Yves Colin, Anastasia Zinchenko, and Florian Hollfelder. Enzyme engineering in biomimetic compartments. *Current Opinion in Structural Biology*, 33:42–51, August 2015. WOS:000365362400007.
- [8] David J. Collins, Adrian Neild, Andrew deMello, Ai-Qun Liu, and Ye Ai. The Poisson distribution and beyond: methods for microfluidic droplet production and single cell encapsulation. *Lab on a Chip*, 15(17):3439–3459, August 2015.

- [9] Dino Di Carlo, Daniel Irimia, Ronald G. Tompkins, and Mehmet Toner. Continuous inertial focusing, ordering, and separation of particles in microchannels. *Proceedings of the National Academy of Sciences of the United States of America*, 104(48):18892–18897, November 2007.
- [10] Jon F. Edd, Dino Di Carlo, Katherine J. Humphry, Sarah KÄ¶ster, Daniel Irimia, David A. Weitz, and Mehmet Toner. Controlled encapsulation of single-cells into monodisperse picolitre drops. *Lab on a Chip*, 8(8):1262–1264, July 2008.
- [11] Jared W Ellefson, Adam J Meyer, Randall A Hughes, Joe R Cannon, Jennifer S Brodbelt, and Andrew D Ellington. Directed evolution of genetic parts and circuits by compartmentalized partnered replication. *Nature biotechnology*, 32(1):97–101, January 2014.
- [12] Andrew D. Ellington and Jack W. Szostak. In vitro selection of RNA molecules that bind specific ligands. *Nature*, 346(6287):818–822, August 1990.
- [13] Ali Fallah-Araghi, Jean-Christophe Baret, Michael Ryckelynck, and Andrew D. Griffiths. A completely in vitro ultrahigh-throughput droplet-based microfluidic screening system for protein engineering and directed evolution. *Lab on a Chip*, 12(5):882–891, 2012. WOS:000300047800006.
- [14] F J Ghadessy, J L Ong, and P Holliger. Directed evolution of polymerase function by compartmentalized self-replication. *Proceedings of the National Academy of Sciences of the United States of America*, 98(8):4552–4557, April 2001.
- [15] Andrew D Griffiths and Dan S Tawfik. Directed evolution of an extremely fast phosphotriesterase by in vitro compartmentalization. *The EMBO journal*, 22(1):24–35, January 2003.
- [16] Evelien W. M. Kemna, Rogier M. Schoeman, Floor Wolbers, Istvan Vermes, David A. Weitz, and Albert van den Berg. High-yield cell ordering and deterministic cell-in-droplet encapsulation using Dean flow in a curved microchannel. *Lab on a Chip*, 12(16):2881–2887, July 2012.
- [17] Milko B. Kermekchiev, Lyubka I. Kirilova, Erika E. Vail, and Wayne M. Barnes. Mutants of Taq DNA polymerase resistant to PCR inhibitors allow DNA amplification from whole blood and crude soil samples. *Nucleic Acids Research*, 37(5):e40, April 2009.
- [18] Balint Kintses, Christopher Hein, Mark F. Mohamed, Martin Fischlechner, Fabienne Courtois, Celine Leine, and Florian Hollfelder. Picoliter Cell Lysate Assays in Microfluidic Droplet Compartments for Directed Enzyme Evolution. *Chemistry & Biology*, 19(8):1001–1009, August 2012. WOS:000309152500012.

- [19] H. Klenow and I. Henningsen. Selective Elimination of the Exonuclease Activity of the Deoxyribonucleic Acid Polymerase from *Escherichia coli* B by Limited Proteolysis*. *Proceedings of the National Academy of Sciences of the United States of America*, 65(1):168–175, January 1970.
- [20] Tadas Povilaitis, Gediminas Alzbutas, Rasa Sukackaite, Juozas Siurkus, and Remigijus Skirgaila. In vitro evolution of phi29 DNA polymerase using isothermal compartmentalized self replication technique. *Protein Engineering, Design and Selection*, 29(12):617–628, December 2016.
- [21] Yannick Rondelez, Guillaume Tresset, Kazuhito V. Tabata, Hideyuki Arata, Hiroyuki Fujita, Shoji Takeuchi, and Hiroyuki Noji. Microfabricated arrays of femtoliter chambers allow single molecule enzymology. *Nature Biotechnology*, 23(3):361–365, March 2005.
- [22] C. Tuerk and L. Gold. Systematic evolution of ligands by exponential enrichment: RNA ligands to bacteriophage T4 DNA polymerase. *Science*, 249(4968):505–510, August 1990.
- [23] Asao Yamauchi, Toshihiro Nakashima, Nobuhiko Tokuriki, Masato Hosokawa, Hideki Nogami, Shingo Arioka, Itaru Urabe, and Tetsuya Yomo. Evolvability of random polypeptides through functional selection within a small library. *Protein Engineering, Design and Selection*, 15(7):619–626, July 2002.
- [24] Anton S. Zadorin and Yannick Rondelez. Natural selection in compartmentalized environment with reshuffling. *arXiv:1707.07461 [q-bio]*, July 2017. arXiv: 1707.07461.
- [25] Anton S. Zadorin and Yannick Rondelez. Selection strategies for randomly distributed replicators. *arXiv:1711.04350 [q-bio]*, November 2017. arXiv: 1711.04350.

Supplemental text

Enrichment factor and selection asymptotics

A. Drame Maigne, A. S. Zadorin, I. Golovkova, Y. Rondelez

November 12, 2018

Contents

1 Enrichment factor is not good for characterization of the selection efficiency	1
2 Initial jump Δ and efficiency comparison	3
3 Examples with P_n different from the Poisson law	4
3.1 Classical selection of polyploid organisms	4
3.2 Random compartmentalization of k -tuplets	4
3.2.1 Compartmentalization in pairs ($k = 2$)	5
3.2.2 Compartmentalization in triplets, quadruplets, etc. ($k > 2$)	5
3.3 Toxicity of multiple encapsulation	6
3.3.1 Critical toxicity	6
3.3.2 Exponential decay	7
4 Polydisperse droplets	7
4.1 General expressions	8
4.2 Monodispersity increases efficiency	9
4.3 Expressions for special distributions	10
4.3.1 Normal distribution	10
4.3.2 Gamma distribution	10
4.3.3 Lognormal distribution	11

1 Enrichment factor is not good for characterization of the selection efficiency

In applications, a popular measure of the selection strength is the so called enrichment factor $\varepsilon \stackrel{\text{def}}{=} \frac{p'}{1-p'} \cdot \frac{1-p}{p}$, where p' is the frequency of the allele of interest after one selection cycle. This value is often used to characterized the efficiency of the enrichment of a functional mutant in a population of dysfunctional wild ones—a typical situation in screening. In this section, we will examin expressions for ε in case of linear and cut-off selection function with or without sharing. These expressions are derived from the update equations for these cases taken from [1].

With the assumption of a population of a functional and a dysfunctional mutants, the linear replication function results in the following expression for ε

$$\varepsilon = 1 + \frac{g(\lambda)}{1 - g(\lambda)} \frac{1}{p},$$

where

$$g(\lambda) \stackrel{\text{def}}{=} \frac{1 - e^{-\lambda}}{\lambda}.$$

As expected, $\varepsilon \rightarrow \infty$, when $\lambda \rightarrow 0$, and $\varepsilon \rightarrow 1$, when $\lambda \rightarrow \infty$. In agreement with the linearizations, at $p \rightarrow 0$ we have $\varepsilon \rightarrow \infty$ and at $p \rightarrow 1$ we have $\varepsilon \rightarrow 1/(1 - g(\lambda)) = \beta^{-1}$, where β is the corresponding multiplier of the linearization of the update equation at $p = 1$.

The linear selection without sharing results in an even simpler expression

$$\varepsilon = 1 + \frac{1}{\lambda p}.$$

The cut-off selection without sharing corresponds to

$$\varepsilon = \frac{1}{1 - e^{-\lambda p}}.$$

Again, $\varepsilon \rightarrow \infty$, when $\lambda \rightarrow 0$ and $p \rightarrow 0$, $\varepsilon \rightarrow 1$, when $\lambda \rightarrow \infty$, and when $p \rightarrow 1$ we have $\varepsilon \rightarrow 1/(1 - e^{-\lambda})$, which is β^{-1} for this case. This expression was originally derived in [2].

Likewise, the cut-off selection with sharing results in

$$\varepsilon = \frac{(1 - p)(e^\lambda - 1)}{(1 - p)e^\lambda + p - e^{\lambda(1-p)}}.$$

As before, $\varepsilon \rightarrow \infty$, when $\lambda \rightarrow 0$ and $p \rightarrow 0$, $\varepsilon \rightarrow 1$, when $\lambda \rightarrow \infty$, and $\varepsilon \rightarrow \beta^{-1}$, when $p \rightarrow 1$, where $\beta = 1 - 1/g(-\lambda)$.

In fact, in general $\varepsilon \rightarrow \alpha$, when $p \rightarrow 0$, and $\varepsilon \rightarrow \beta^{-1}$, when $p \rightarrow 1$, where α is the multiplier of the linearization of the update equation in the vicinity of $p = 0$. As ε depends on p , it is not a good measure of the efficiency of the selection process by itself. But even a pair (p, ε) does not well characterize the selection, as the dependence of ε on p may be very different, as it is seen from the examples above. A complete characterization would be given by the entire curve $\varepsilon(p)$. However, gathering this information is very costly experiment-wise. An alternative could be the measurement of the asymptotic behaviour at $p = 0$ and at $p = 1$ and some interpolation in-between.

In reality, when a rare functional mutant is selected from a population of dysfunctional ones, only the asymptotics at $p = 0$ is relevant. Furthermore, as we have seen, the multiplier α of the linearization at this point is not informative, as the linearization itself is not defined ($\alpha = \infty$). This happens because the curve $p'(p)$ becomes discontinuous at $p = 0$. Although $p'(0) = 0$, the limit $\Delta \stackrel{\text{def}}{=} \lim_{p \rightarrow 0} p'(p)$ is positive, which reflects the effortless invasion of the population of dysfunctional mutants by a functional one. Therefore, this jump Δ is itself a good characteristic of the selection efficiency in such a case (see Figure 1).

The corresponding asymptotics of $p'(p)$ at $p \rightarrow 0$ up to the linear term is given below for all the cases we discussed before. The linear selection function with sharing:

$$p' = g(\lambda) + (1 - g(\lambda))p. \quad (1)$$

The linear selection without sharing:

$$p' = \frac{1}{1 + \lambda} + \frac{\lambda}{1 + \lambda} p. \quad (2)$$

The cut-off selection without sharing (screening):

$$p' = \frac{1}{1 + \lambda} + \frac{\lambda(2 + \lambda)}{2(1 + \lambda)^2} p + o(p). \quad (3)$$

The cut-off selection with sharing:

$$p' = g(\lambda) + \frac{1 - e^{-\lambda}}{2} p + o(p). \quad (4)$$

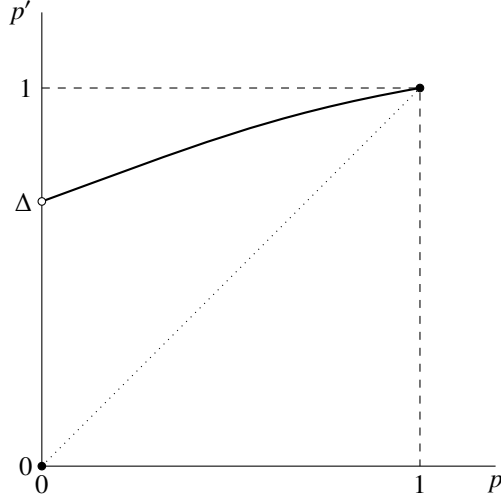


Figure 1: A sketch of a typical function $p'(p)$ (the thick line) for a fixed value of λ , $0 < \lambda < \infty$, for a mixed population of a functional mutant with frequency p and of a dysfunctional one with frequency $1 - p$.

2 Initial jump Δ and efficiency comparison

Equations (1–4) show an interesting tendency. The value of Δ does not depend on the replication function. It only depends on the offspring sharing rule. It appears that this is a general property.

For a general replication function f , a general sharing rule $\varphi(n)$ (the fraction of the value given by f allocated to each individual in the droplet of size n), and a general phenotypic distribution ρ , the update equation is given by (see [3])

$$\rho' = \frac{\sum_n P_n n \varphi(n) \langle \delta_x * \rho^{*n-1}, f \rangle}{\sum_n P_n n \varphi(n) \langle \rho^{*n}, f \rangle} \rho.$$

Here probability distributions are treated as generalized functions (Schwartz' distributions, linear continuous functionals on continuous functions with finite support) and $\langle \rho, \varphi \rangle$ means the action of distribution ρ on function φ . The asterisk means convolution and ρ^{*n} means the n th convolutional power. δ_x means δ -function concentrated at x . P_n is the probability to find n individuals in a compartment.

In the case of a mix of a lethal phenotype and a functional one with value x , we have $\rho = (1 - p)\delta_0 + p\delta_x$, $\rho' = (1 - p')\delta_0 + p'\delta_x$, $f(0) = 0$, and we are interested in looking at the term with δ_x at the next step of selection to determine p' . One can show that in this case, for f that does not grow too steeply, we have the following limit

$$\frac{\sum_n P_n n \varphi(n) \langle \delta_x * \rho^{*n-1}, f \rangle}{\sum_n P_n n \varphi(n) \langle \rho^{*n}, f \rangle} p \delta_x \rightarrow \frac{\sum_n P_n n \varphi(n)}{\sum_n P_n n^2 \varphi(n)} \delta_x, \quad p \rightarrow 0.$$

And therefore, we have, for a general partition rule P_n ,

$$\Delta = \frac{\sum_n P_n n \varphi(n)}{\sum_n P_n n^2 \varphi(n)}. \quad (5)$$

For the Poisson law $P_n = e^{-\lambda} \lambda^n / n!$ we have

$$\Delta = \frac{\sum_{n=0}^{\infty} \frac{\lambda^n}{n!} \varphi(n+1)}{\sum_{n=0}^{\infty} \frac{\lambda^n}{n!} (n+1) \varphi(n+1)}. \quad (6)$$

This stays true even for a nonadditive mixing of activities (provided sufficiently limited growth of the replication function with the number of individuals in a droplet and with their activities). Here the update equation takes the form (see [3])

$$\rho' = \frac{\sum_n P_n n \langle \delta_x \otimes \rho^{\otimes n-1}, f_n \rangle}{\sum_n P_n n \langle \rho^{\otimes n}, f_n \rangle} \rho. \quad (7)$$

Here $f_n: \mathbb{R}^n \rightarrow \mathbb{R}$ are the functions that encode return the per-individual fitness to n phenotypic activities of coencapsulated individuals and \otimes means the tensor product of distributions.

If we now assume $\rho = (1-p)\delta_0 + p\delta_x$, $f_n(0, \dots, 0) = 0$, $f_n(x, 0, \dots, 0) = \varphi(n)$, then we recover (5) in the limit $p \rightarrow 0$.

For the selection with sharing we have $\varphi(n) = 1/n$, and thus (6) gives $\Delta = g(\lambda)$, regardless of f . Without sharing we have $\varphi(n) = 1$, and thus $\Delta = 1/(1+\lambda)$. In the case of sharing both the activity and the offspring, we have $\varphi(n) = 1/n^2$, and thus $\Delta = (\text{Ei}(\lambda) - \ln \lambda - \gamma)/(e^\lambda - 1)$, where Ei is the exponential integral and γ is Euler's constant.

We can conclude that, if the sharing behaviour is known in the experiment, one can obtain the theoretically expected ideal macroscopic gene frequency jump Δ after one round of selection of a very rare functional mutant in a population of dysfunctional ones. This Δ can be used as a benchmark for the comparison of the experimental protocol efficiency. The advantage of this value is its independence of the replication function f .

3 Examples with P_n different from the Poisson law

We will illustrate how to apply (5) to some cases of non-Poissonian partitioning P_n . In particular, we will show how the well known case of a polyploid population (with no recombination) is recovered from the general formula, we will also discuss what changes if only pairs, triples, etc. are randomly encapsulated. The latter situation corresponds either to 'sticking' of haploid individuals (for instance in pairs, triples, tetrads, etc.) or to random encapsulation of polyploid individuals, when the total droplet phenotype depends only on the total chromosomal composition regardless the origin of each chromosome. Finally, we will consider the inhibition of replication by multiple encapsulation.

3.1 Classical selection of polyploid organisms

Consider $P_n = \delta_{kn}$, where δ_{kn} is the Kronecker delta. This means that each droplet contains exactly k individuals. In this case, the droplets effectively behave as k -ploid organisms, where individuals play role of (single locus) chromosomes inside droplets and that of gamets during the redistribution.

It is intuitively clear what to expect from the selection of a rare functional mutation in such situation. Indeed, any droplet that contains a functional gene also contains $k-1$ dysfunctional ones in the limit $p \rightarrow 0$. Therefore, after selection we will have $p' = 1/k$, and thus, $\Delta = 1/k$. As expected, when $P_n = \delta_{kn}$ is substituted to (5), we get the same result regardless of φ :

$$\Delta = \frac{k\varphi(k)}{k^2\varphi(k)} = \frac{1}{k}. \quad (8)$$

3.2 Random compartmentalization of k -tuplets

The case of a random compartmentalization of k -tuplets of individuals corresponds to

$$P_n = \begin{cases} \mathcal{N} \frac{\lambda^n}{n!}, & n \equiv 0 \pmod{k}, \\ 0, & n \not\equiv 0 \pmod{k}, \end{cases}$$

where \mathcal{N} is the normalization constant. Let us also denote $\tilde{P}_n \stackrel{\text{def}}{=} P_n/\mathcal{N}$. It is clear, that Δ can also be computed as

$$\Delta = \frac{\sum_n \tilde{P}_n n \varphi(n)}{\sum_n \tilde{P}_n n^2 \varphi(n)}. \quad (9)$$

To find the expression for Δ with both $\varphi(n) = 1/n$ (sharing) and $\varphi(n) = 1$ (no sharing), it is enough to find

$$\Sigma \stackrel{\text{def}}{=} \sum_n \tilde{P}_n, \quad \langle n \rangle \stackrel{\text{def}}{=} \sum_n \tilde{P}_n n, \quad \text{and} \quad \langle n^2 \rangle \stackrel{\text{def}}{=} \sum_n \tilde{P}_n n^2.$$

(As a matter of fact, $\mathcal{N} = \Sigma$.) Then Δ can be written in the following way:

$$\Delta = \frac{\Sigma - 1}{\langle n \rangle} \text{ with sharing;} \quad \Delta = \frac{\langle n \rangle}{\langle n^2 \rangle} \text{ without sharing.}$$

The following expressions, which can be proved by termwise differentiation of Σ in λ , are also useful:

$$\langle n \rangle = \lambda \frac{d}{d\lambda} \Sigma, \quad \langle n^2 \rangle = \left(\lambda^2 \frac{d^2}{d\lambda^2} + \lambda \frac{d}{d\lambda} \right) \Sigma. \quad (10)$$

3.2.1 Compartmentalization in pairs ($k = 2$)

In this case we have

$$\Sigma = \sum_{n=0}^{\infty} \frac{\lambda^{2n}}{(2n)!} = \text{ch } \lambda, \quad (11)$$

where $\text{ch } x \stackrel{\text{def}}{=} (e^x + e^{-x})/2$ is the hyperbolic cosine. Using (10), we find

$$\langle n \rangle = \lambda \text{ sh } \lambda, \quad \langle n^2 \rangle = \lambda^2 \text{ ch } \lambda + \lambda \text{ sh } \lambda,$$

where $\text{sh } x \stackrel{\text{def}}{=} (e^x - e^{-x})/2$ is the hyperbolic sine. Therefore, we have

$$\Delta = \frac{\text{ch } \lambda - 1}{\lambda \text{ sh } \lambda} \text{ with sharing;} \quad \Delta = \frac{\text{th } \lambda}{\lambda + \text{th } \lambda} \text{ without sharing,} \quad (12)$$

where $\text{th } x \stackrel{\text{def}}{=} \text{sh } x / \text{ch } x$ is the hyperbolic tangent.

3.2.2 Compartmentalization in triplets, quadruplets, etc. ($k > 2$)

For a given k consider complex k th roots of unity, that is complex numbers z such that $z^k = 1$. There are exactly k different roots and they all have the form $z = e^{2\pi i m/k}$, where $m \in \mathbb{Z}$ and i is the imaginary unit (of course, only $m \in \{0, 1, \dots, k-1\}$ are essential). They possess a simple but useful property valid for any $l \in \mathbb{Z}$:

$$\sum_{m=0}^{k-1} \left(e^{2\pi i m/k} \right)^l = 1 + e^{2\pi i l/k} + e^{2\pi i 2l/k} + \dots + e^{2\pi i (k-1)l/k} = \begin{cases} k, & l \equiv 0 \pmod{k}, \\ 0, & l \not\equiv 0 \pmod{k}. \end{cases}$$

This property allows to express \tilde{P}_n in the following form

$$\tilde{P}_n = \frac{1}{k} \sum_{m=0}^{k-1} \frac{(\lambda e^{2\pi im/k})^n}{n!}.$$

Now Σ splits into k individual sums each of which results in a simple exponential function

$$\Sigma = \frac{1}{k} \sum_{n=0}^{\infty} \sum_{m=0}^{k-1} \frac{(\lambda e^{2\pi im/k})^n}{n!} = \frac{1}{k} \sum_{m=0}^{k-1} e^{\lambda e^{2\pi im/k}}$$

In fact, this was already secretly used in (11), where we have $\{e^{2\pi im/2}\} = \{1, -1\}$, and thus, $\Sigma = (e^\lambda + e^{-\lambda})/2$. Using (10), we find

$$\langle n \rangle = \frac{\lambda}{k} \sum_{m=0}^{k-1} e^{2\pi im/k} e^{\lambda e^{2\pi im/k}}, \quad \langle n^2 \rangle = \frac{\lambda^2}{k} \sum_{m=0}^{k-1} e^{4\pi im/k} e^{\lambda e^{2\pi im/k}} + \frac{\lambda}{k} \sum_{m=0}^{k-1} e^{2\pi im/k} e^{\lambda e^{2\pi im/k}}.$$

Finally, the the general expression for Δ in case of an arbitrary k is

$$\Delta = \frac{\sum_{m=0}^{k-1} e^{\lambda e^{2\pi im/k}} - k}{\lambda \sum_{m=0}^{k-1} e^{2\pi im/k} e^{\lambda e^{2\pi im/k}}} \text{ with sharing; } \quad \Delta = \frac{\sum_{m=0}^{k-1} e^{2\pi im/k} e^{\lambda e^{2\pi im/k}}}{\sum_{m=0}^{k-1} e^{2\pi im/k} e^{\lambda e^{2\pi im/k}} (1 + \lambda e^{2\pi im/k})} \text{ without sharing.} \quad (13)$$

It is not difficult to show that $\Delta \rightarrow k^{-1}$, as $\lambda \rightarrow 0$ (reduction to the k -ploid case (8)), and $\Delta \sim \lambda^{-1}$, as $\lambda \rightarrow \infty$. It is also easy to check that the cases $k = 1$ (the Poisson partitioning) and $k = 2$ (the Poisson partitioning of pairs) are correctly recovered from (13). Indeed, with $k = 1$, we have $\{e^{2\pi im/k}\} = \{1\}$ and $\Delta = (e^\lambda - 1)/(\lambda e^\lambda) = g(\lambda)$ with sharing, $\Delta = 1/(1 + \lambda)$ without. With $k = 2$, we have $\{e^{2\pi im/k}\} = \{1, -1\}$ and (13) turns into (12).

Let us also consider the case of triplets, where we have $k = 3$. The set of 3th roots of unity is equal to $\{e^{2\pi im/3}\} = \{1, (-1 + i\sqrt{3})/2, (-1 - i\sqrt{3})/2\}$, and thus, after simplification

$$\sum_{m=0}^2 e^{\lambda e^{2\pi im/3}} = e^\lambda + 2e^{-\lambda/2} \cos \frac{\lambda\sqrt{3}}{2}.$$

By differentiation, we find

$$\sum_{m=0}^2 e^{2\pi im/3} e^{\lambda e^{2\pi im/3}} = \frac{d}{d\lambda} \sum_{m=0}^2 e^{\lambda e^{2\pi im/3}} = e^\lambda - e^{-\lambda/2} \left(\sqrt{3} \sin \frac{\lambda\sqrt{3}}{2} + \cos \frac{\lambda\sqrt{3}}{2} \right),$$

and

$$\sum_{m=0}^2 e^{4\pi im/3} e^{\lambda e^{2\pi im/3}} = \frac{d^2}{d\lambda^2} \sum_{m=0}^2 e^{\lambda e^{2\pi im/3}} = e^\lambda + e^{-\lambda/2} \left(\sqrt{3} \sin \frac{\lambda\sqrt{3}}{2} - \cos \frac{\lambda\sqrt{3}}{2} \right).$$

And finally,

$$\Delta = \frac{e^\lambda + 2e^{-\lambda/2} \cos \frac{\lambda\sqrt{3}}{2} - 3}{\lambda \left(e^\lambda - e^{-\lambda/2} \left(\sqrt{3} \sin \frac{\lambda\sqrt{3}}{2} + \cos \frac{\lambda\sqrt{3}}{2} \right) \right)}, \text{ with sharing}$$

and

$$\Delta = \frac{e^{3\lambda/2} - \sqrt{3} \sin \frac{\lambda\sqrt{3}}{2} - \cos \frac{\lambda\sqrt{3}}{2}}{(\lambda + 1) \left(e^{3\lambda/2} - \cos \frac{\lambda\sqrt{3}}{2} \right) + \sqrt{3}(\lambda - 1) \sin \frac{\lambda\sqrt{3}}{2}}, \text{ without sharing.}$$

3.3 Toxicity of multiple encapsulation

Sometimes the inclusion of too many individuals (of any genotype) in a compartment can inhibit the downstream replication. This situation arises, when, for example, the compartments are droplets of an emulsion and the genes (genomes) and their products (phenotypic manifestation) are delivered by bacterial cells. If the bacteria are lysed inside the droplets and their content is inhibiting to the subsequent steps, the replication efficiency will drop with the increase of the number of coencapsulated bacteria.

Although this case is not purely a case of P_n different from the Poisson law, and it rather modifies $\varphi(n)$, it nevertheless can be mathematically considered as modifying P_n . Indeed, in this case the regular sharing rule $\varphi(n)$ in (5) is modified by the toxicity factor $\varphi(n) \mapsto t(n)\varphi(n)$ (see (7)). However, what is important is the product $P_n t(n)\varphi(n)$, therefore, one can equivalently use the modification $P_n \mapsto P_n t(n)$, keeping the sharing rule $\varphi(n)$ the same.

We will consider only two simple cases of this phenomenon: 1) when the replication is not influenced, if the number of individual does not surpass some critical number k , and it is completely inhibited otherwise, and 2) when the replication efficiency decays exponentially, $t(n) = d^{-n}$.

3.3.1 Critical toxicity

In this case we have $P_n \sim \lambda^n/n!$, when $n \leq k$, and $P_n = 0$ otherwise. After a simple algebraic rearrangement, using (5), we conclude

$$\Delta = \frac{e_k(\lambda) - 1}{\lambda e_{k-1}(\lambda)} \quad \text{with sharnig}; \quad \Delta = \frac{1}{1 + \lambda \frac{e_{k-2}(\lambda)}{e_{k-1}(\lambda)}} \quad \text{without sharing},$$

where

$$e_k(x) \stackrel{\text{def}}{=} \sum_{n=0}^k \frac{x^n}{n!}$$

is the truncated Taylor expansion of the exponential function.

Note that $\Delta \rightarrow 1$, as $\lambda \rightarrow 0$, and $\Delta \rightarrow k^{-1}$ as $\lambda \rightarrow \infty$, as it should be. Indeed, when λ is very large, the compartments with functional replication are dominated by the ones with k individuals, and we have a convergence to the k -ploid case.

In particular, two practically interesting cases are $k = 2$ and $k = 3$ ($k = 1$ effectively means no cocompartmentalization, and $k > 3$ is difficult to justify theoretically). For $k = 2$ we have

$$\Delta = \frac{1}{2} \frac{2 + \lambda}{1 + \lambda} \quad \text{with sharnig}; \quad \Delta = \frac{1 + \lambda}{1 + 2\lambda} \quad \text{without sharing},$$

while for $k = 3$ we have

$$\Delta = \frac{1}{3} \frac{6 + 3\lambda + \lambda^2}{2 + 2\lambda + \lambda^2} \quad \text{with sharnig}; \quad \Delta = \frac{2 + 2\lambda + \lambda^2}{2 + 4\lambda + 3\lambda^2} \quad \text{without sharing}.$$

3.3.2 Exponential decay

Consider that the replication efficiency decays by the same factor $d > 1$ with every individual added to a compartment. In this case we have $P_n \sim d^{-n}\lambda^n/n!$, and the resulting expressions are immediately derived noticing that this is equivalent to a simple change of λ ($\lambda \mapsto \lambda/d$)

$$\Delta = g(\lambda/d) \quad \text{with sharnig}; \quad \Delta = \frac{d}{d + \lambda} \quad \text{without sharing}.$$

4 Polydisperse droplets

Let us consider the case of random compartmentalization but with compartments that vary in size. Let us first suppose that there are in total M compartments (of all sizes) and N individuals. Then we can define the bulk occupancy

$$\tilde{\lambda} \stackrel{\text{def}}{=} \frac{N}{M}.$$

Let us in addition suppose that there are finite number of size (volume) classes of compartments. A class j is characterized by the compartment volume v_j and the number of its members M_j ($\sum_j M_j = M$). If the classes are large enough and if the individuals are homogeneously spread in the encapsulated solution, the number of individuals in all the j th class compartments is equal to $N_j = v_j M_j N / \sum_k v_k M_k$ ($\sum_j N_j = N$), that is this number constitutes the same part of the total N as the part that the volume of all the j th compartments takes in the total volume of all compartments. Let us introduce the mean number of individuals in a compartment of class j

$$\lambda_j \stackrel{\text{def}}{=} \frac{N_j}{M_j} = \frac{\tilde{\lambda}}{\bar{v}} v_j, \quad \text{where} \quad \bar{v} = \frac{\sum_j v_j M_j}{M}. \quad (14)$$

The value λ_j serves as the local Poisson parameter for the individuals redistribution law in the j th class of droplets. More specifically, the probability to find n individuals in a randomly chosen compartment of class j (with the volume v_j) is (exactly or approximately in the limit of large population and compartments number in each class, depending on the protocol of the compartmentalization) equal to $e^{-\lambda_j} \lambda_j^n / n!$.

Another observations important for the following is that if p_j is the probability for a randomly chosen *compartment* to be in class j ($p_j = M_j/M$) and q_j is the probability for a randomly chosen *individual* to be in class j ($q_j = N_j/N$), then they are related by

$$q_j = \frac{N_j}{N} = \frac{v_j}{\bar{v}} \frac{M_j}{M} = \frac{v_j}{\bar{v}} p_j, \quad (15)$$

or simply by $q_j \sim v_j p_j$ and, taking into account (14), $q_j \sim \lambda_j p_j$.

4.1 General expressions

Now we will generalize this to an arbitrary compartment volume distribution in the following way. Let the distribution of *compartments* by the volume be given by the probability density $\omega(v)$. For instance, the preceding example corresponds to $\omega = \sum_j p_j \delta_{v_j}$. As before, we denote the mean volume of compartments by $\bar{v} = \langle \omega(v), v \rangle$.

Then λ is distributed in the ensemble of *compartments* according to the probability density $F_* \omega$, where F_* is the pushforward of the function $F: x \mapsto x \tilde{\lambda} / \bar{v}$, so for any test function φ we have $\langle F_* \omega, \varphi \rangle = \langle \omega, \varphi \circ F \rangle$. In particular, $\tilde{\lambda}$ is the mean of $F_* \omega$. According to (15), the distribution Λ of λ in the population of *individuals* is then equal to

$$\Lambda(\lambda) = \frac{\lambda F_* \omega(\lambda)}{\langle \lambda F_* \omega(\lambda), 1 \rangle} = \frac{\lambda}{\tilde{\lambda}} F_* \omega(\lambda) = \frac{\bar{v}}{\tilde{\lambda}^2} \lambda \omega\left(\frac{\bar{v}}{\tilde{\lambda}} \lambda\right). \quad (16)$$

Let us denote $\bar{\lambda}^n_\Lambda \stackrel{\text{def}}{=} \langle \Lambda(\lambda), \lambda^n \rangle$, and thus $\bar{\lambda}_\Lambda = \langle \Lambda(\lambda), \lambda \rangle$, and in general $\overline{\Phi(\lambda)}_\Lambda \stackrel{\text{def}}{=} \langle \Lambda(\lambda), \Phi(\lambda) \rangle$ (the subscript Λ is kept not to forget that all the averages are taken over the *population of individuals* and not over the ensemble of compartments). Then it is easy to show that

$$\bar{\lambda}_\Lambda = \tilde{\lambda} \frac{\bar{v}^2}{\bar{v}^2}, \quad \text{and in general} \quad \bar{\lambda}^n_\Lambda = \tilde{\lambda}^n \frac{\bar{v}^{n+1}}{\bar{v}^{n+1}}, \quad (17)$$

where \bar{v}^n is the n th moment of ω : $\bar{v}^n \stackrel{\text{def}}{=} \langle \omega(v), v^n \rangle$.

To find Δ , we have to rewrite (7) for polydisperse compartments. The structure of the formula is the following

$$\rho'(x) = \frac{\text{mean fitness of genotype } x}{\text{mean population fitness}} \rho(x) = \frac{\langle w_x \rangle}{\langle w \rangle} \rho(x).$$

Let us denote $P_n(\lambda) \stackrel{\text{def}}{=} e^{-\lambda} \lambda^n / n!$. For a given subpopulation with a given λ , the mean fitness of genotype x is equal to (see [3])

$$\langle w_x(\lambda) \rangle = \frac{\sum_n P_n(\lambda) n \langle \delta_x \otimes \rho^{\otimes n-1}, f_n \rangle}{\sum_n P_n(\lambda) n} = \frac{1}{\lambda} \sum_n P_n(\lambda) n \langle \delta_x \otimes \rho^{\otimes n-1}, f_n \rangle,$$

while the mean subpopulation fitness is equal to

$$\langle w(\lambda) \rangle = \frac{\sum_n P_n(\lambda) n \langle \rho^{\otimes n}, f_n \rangle}{\sum_n P_n(\lambda) n} = \frac{1}{\lambda} \sum_n P_n(\lambda) n \langle \rho^{\otimes n}, f_n \rangle.$$

The total population mean fitness of genotype x and the total overall population fitness are obtained from these values by averaging in λ : $\langle w_x \rangle = \overline{\langle w_x(\lambda) \rangle}_\Lambda$, $\langle w \rangle = \overline{\langle w(\lambda) \rangle}_\Lambda$. Therefore, with $\rho = (1-p)\delta_0 + p\delta_x$ and with the same assumptions and using the same method, as in Section 2, in the limit $p \rightarrow 0$ we obtain

$$\Delta = \frac{\overline{\left(\lambda^{-1} \sum_n P_n(\lambda) n \varphi(n) \right)}_\Lambda}{\overline{\left(\lambda^{-1} \sum_n P_n(\lambda) n^2 \varphi(n) \right)}_\Lambda}. \quad (18)$$

We will again consider only cases $\varphi(n) = 1/n$ (sharing) and $\varphi(n) = 1$ (no sharing). With sharing, in the numerator of (18) we have $g(\lambda)$ averaged over λ , and in the denominator we have 1. Without sharing, in the numerator we have 1 and in the denominator we have $(\lambda + \lambda^2)/\lambda = 1 + \lambda$ averaged over λ . Therefore, we have

$$\Delta = \overline{g(\lambda)}_\Lambda, \quad \text{with sharing}; \quad \Delta = \frac{1}{1 + \tilde{\lambda}_\Lambda}, \quad \text{without sharing}.$$

Let us rewrite these quantities in terms of the volume distribution in compartments ω , which is linked to Λ by (16). In the case of sharing, we have

$$\Delta = \overline{g(\lambda)}_\Lambda = \left\langle \frac{\lambda}{\tilde{\lambda}} F_* \omega(\lambda), \frac{1 - e^{-\lambda}}{\lambda} \right\rangle = \left\langle F_* \omega(\lambda), \frac{1 - e^{-\lambda}}{\tilde{\lambda}} \right\rangle = \left\langle \omega(v), \frac{1 - e^{-\tilde{\lambda}v/\bar{v}}}{\tilde{\lambda}} \right\rangle = \frac{1 - \psi_\omega(-\tilde{\lambda}/\bar{v})}{\tilde{\lambda}}, \quad (19)$$

where $\psi_\omega(y) \stackrel{\text{def}}{=} \langle \omega(x), e^{xy} \rangle$ is the moment generating function of ω .

The case without sharing is even simpler. Here we obtain, using (17)

$$\Delta = \frac{1}{1 + \tilde{\lambda} \bar{v}^2 / \bar{v}^2}. \quad (20)$$

4.2 Monodispersity increases efficiency

There are two general ways of how the water-in-oil emulsion for compartmentalized evolutionary experiments is generated: 1) shaking of the bulk mixture of genome carrier containing solution and oil resulting in a significantly polydisperse emulsion and 2) generation of a monodisperse emulsion with microfluidics. As the shaking is simpler than the microfluidic approach, it is interesting to know, if there are any benefits to the latter. We will see that polydispersity (shaking) indeed worsens the selection efficiency. More precisely, of two emulsions, a polydisperse and a monodisperse ones, with the same bulk $\tilde{\lambda}$ and the same average droplet volume \bar{v} (it is just the droplet volume for the monodisperse emulsion) the polydisperse emulsion always has Δ not larger than the monodisperse one.

We will only consider the case with sharing and the case without sharing, as before. In the monodisperse case we have the volume distribution given by $\delta_{\bar{v}}$. Let us denote the volume distribution of the polydisperse case by ω and let us keep all the notations associated with ω that were introduced previously. With no sharing, according to (20), we have

$$\Delta_{\text{polydisperse}} = \frac{1}{1 + \tilde{\lambda} \bar{v}^2 / \bar{v}^2} \leq \frac{1}{1 + \tilde{\lambda}} = \Delta_{\text{monodisperse}},$$

as for any ω we have $\bar{v}^2 \geq \bar{v}^2$.

With sharing, so called Jensen's inequality can be used, which states the following. Consider any probability distribution ρ and any convex on $\text{supp } \rho$ function φ , that is for any μ such that $0 \leq \mu \leq 1$ and any x_1 and x_2 from $\text{supp } \rho$ we have

$$\varphi(\mu x_1 + (1 - \mu)x_2) \leq \mu \varphi(x_1) + (1 - \mu)\varphi(x_2).$$

Then Jensen's theorem states that the following holds

$$\varphi(\bar{x}_\rho) \leq \overline{\varphi(x)_\rho}.$$

In words, the mean of the convex function is larger than the value of the function of the mean. As e^x is a convex function of x , we conclude from (19) that $\psi_\omega(y) \geq e^{y\bar{v}}$ and

$$\Delta_{\text{polydisperse}} = \frac{1 - \psi_\omega(-\tilde{\lambda}/\bar{v})}{\tilde{\lambda}} \leq \frac{1 - e^{-\tilde{\lambda}}}{\tilde{\lambda}} = g(\tilde{\lambda}) = \Delta_{\text{monodisperse}}.$$

Using the fact that $g(\lambda)$ itself is a convex function, we conclude, by Jensen's inequality, that

$$\overline{g(\lambda)_\Lambda} \geq g(\bar{\lambda}_\Lambda) = g(\tilde{\lambda} \bar{v}^2 / \bar{v}^2),$$

where Λ is the distribution of λ in the population for the polydisperse case (in the monodisperse case this distribution is given by $\delta_{\tilde{\lambda}}$). Therefore, we have an estimate from above on the gain in Δ due to switching to a monodisperse emulsion in the case of sharing

$$\Delta_{\text{mododisperse}} - \Delta_{\text{polydisperse}} \leq g(\tilde{\lambda}) - g(\tilde{\lambda} \bar{v}^2 / \bar{v}^2).$$

4.3 Expressions for special distributions

Usually, the experimentally compartment size distribution is fit with some common distribution with few parameters. Therefore, it would be interesting to see, how the efficiency of selection depends on these parameters. We will assume that the compartments are spherical droplets of an emulsion. We will only consider the normal distribution, the Gamma distribution, and the lognormal distribution of both radii and volumes.

4.3.1 Normal distribution

If volumes are distributed normally with mean μ and standard deviation σ , thus with the density function

$$\omega(v) = \frac{1}{\sqrt{2\pi}\sigma} \exp\left(-\frac{(v - \mu)^2}{2\sigma^2}\right),$$

so $\bar{v} = \mu$, then we have

$$\Delta = \frac{1 - e^{-\tilde{\lambda}} e^{\tilde{\lambda}^2 \frac{\sigma^2}{2\mu^2}}}{\tilde{\lambda}} \quad \text{with sharing,} \quad \Delta = \frac{1}{1 + \tilde{\lambda} \left(1 + \frac{\sigma^2}{\mu^2}\right)} \quad \text{without sharing.}$$

It must be noted that the normal distribution can adequately represent the volume distribution only for $\sigma \ll \mu$. With $\sigma \gtrsim \mu$, a significant portion of the distribution represents unphysical negative volumes.

In applications, however, it is the radii distribution which is measured instead of the volume distribution. Let the droplet radii r be distributed normally with mean radius μ_r and the standard deviation σ_r . Then, without sharing, one has

$$\Delta = \frac{1}{1 + \tilde{\lambda}R}, \quad (21)$$

where

$$R = \frac{\overline{r^6}}{\overline{r^3}^2} = \frac{\mu_r^6 + 15\mu_r^4\sigma_r^2 + 45\mu_r^2\sigma_r^4 + 15\sigma_r^6}{(\mu_r^3 + 3\mu_r\sigma_r^2)^2}.$$

Unfortunately, the pure normal distribution of radii is not adequate for the case with sharing, as the Laplace transform of the corresponding volume distribution diverges.

4.3.2 Gamma distribution

Gamma distribution, which is given by

$$\omega(v) = \frac{v^{\alpha-1}}{\Gamma(\alpha)\theta^\alpha} e^{-v/\theta},$$

and which has two parameters, too (the shape parameter α and the scale parameter θ), has two advantages with respect to the normal distribution: it does not have the negative part and it is skewed, which better fits empirical cases. In this case, the mean volume is equal to $\bar{v} = \alpha\theta$, the n -th moment is equal to $\overline{v^n} = \alpha(\alpha+1) \dots (\alpha+n-1)\theta^n$, and the Laplace transform of the distribution is equal to $\mathcal{L}[\omega](x) = \psi_\omega(-x) = (1 + \theta x)^{-\alpha}$. Therefore, we obtain

$$\Delta = \frac{1 - \left(1 + \frac{\tilde{\lambda}}{\alpha}\right)^{-\alpha}}{\tilde{\lambda}} \quad \text{with sharing}, \quad \Delta = \frac{1}{1 + \tilde{\lambda}\frac{\alpha+1}{\alpha}} \quad \text{without sharing}.$$

Note that these distributions do not depend on θ .

If the radius, instead, is well fit with the gamma distribution

$$q(r) = \frac{r^{\alpha_r-1}}{\Gamma(\alpha_r)\theta_r^{\alpha_r}} e^{-r/\theta_r},$$

then, for the case of no sharing, Δ is given by (21) with

$$R = \frac{(\alpha_r + 3)(\alpha_r + 4)(\alpha_r + 5)}{\alpha_r(\alpha_r + 1)(\alpha_r + 2)}.$$

We were not able to express Δ in a closed form for the case of sharing.

4.3.3 Lognormal distribution

Finally, many empirical distributions of the droplet size in emulsions are well fit with lognormal distribution given by

$$\omega(v) = \frac{1}{\sqrt{2\pi v\sigma}} \exp\left(-\frac{(\ln v - \mu)^2}{2\sigma^2}\right), \quad (22)$$

For this distribution, we have $\overline{v^n} = e^{n\mu+n^2\sigma^2/2}$. Therefore, we conclude that with no sharing we have

$$\Delta = \frac{1}{1 + \tilde{\lambda}e^{\sigma^2}}.$$

This value does not depend on μ .

Unfortunately, there is no known closed form expression for the Laplace transform of the lognormal distribution.

It is the radius distribution that is usually empirically fit with the lognormal distribution. However, as this distribution family is invariant under the variable change of the form $x \mapsto x^\alpha$, it is only necessary to know how to derive σ for the volume distribution knowing the radial distribution. Let the radius be distributed with the density function

$$g(r) = \frac{1}{\sqrt{2\pi r}\sigma_r} \exp\left(-\frac{(\ln r - \mu_r)^2}{2\sigma_r^2}\right).$$

Then, as $v = \frac{4}{3}\pi r^3$, the volume is distributed as (22) with $\sigma = 3\sigma_r$ and $\mu = 3\mu_r + \ln \frac{4\pi}{3}$.

References

- [1] Zadorin, A.S. and Rondelez, Y., 2017. Selection strategies for randomly distributed replicators. arXiv preprint arXiv:1711.04350.
- [2] Baret, J.C., Miller, O.J., Taly, V., Rycelynck, M., El-Harrak, A., Frenz, L., Rick, C., Samuels, M.L., Hutchison, J.B., Agresti, J.J. and Link, D.R., 2009. Fluorescence-activated droplet sorting (FADS): efficient microfluidic cell sorting based on enzymatic activity. *Lab on a Chip*, 9(13), pp.1850-1858.
- [3] Zadorin, A.S. and Rondelez, Y., 2017. Natural selection in compartmentalized environment with reshuffling. arXiv preprint arXiv:1707.07461.

SI Material & Methods

Quantifying the performance of high-throughput directed evolution protocols

Adèle Dramé-Maigné*, Anton Zadorin*, Iaroslava Golovkova, Yannick Rondelez

Mock selection of the KlenTaq polymerase

Compartmentalized selection with various λ

For mock selection experiments, an inactive version of the KlenTaq polymerase was constructed via site-directed mutagenesis (Q5® Site-Directed Mutagenesis Kit from NEB) using the following primers:

Pr_NegMut_Fwd: 5'-GGTTGCACTGGGTATAGCCAG

Pr_NegMut_Rw: 5'-AGCAGCCAACCTTCTTCGG

The aspartic acid 332 (GAT) was changed into a glycine (GGT) in the DYSQIELR motif (reference motif).

Bacteria expressing either a wild-type or the inactivated version of the KlenTaq polymerase was grown and induced at 37°C and 250 rpm for 2 hours with 0.1% of L-rhamnose. After induction, the bacteria were pelleted in a centrifuge at 5000 g for 5min. They were washed (resuspended and centrifuged 5min at 5000 g) twice in a resuspension buffer (Tris-HCl pH 7.5 50mM, NaCl 100 mM). A solution was then prepared containing Thermopol DF buffer (NEB) (1x) with 1.5mM MgSO₄, 400 µg/mL of BSA9000S (NEB), 200 µM of each dNTPs (NEB), 1ng/µL of Yeast RNA (Merck), 0.4% of Pluronic F-127 (Sigma-Aldrich) and the bacteria. We add 200nM of primers:

reverse: 5'-TTAGGTCTACTAAGCAAAAAACCCCTC

forward: 5'-TTAGGTCTCATCTATAATACGACTCACTATAGGGAG

Bacteria concentration was determined using OD600 measurement. The ratio of active over inactive bacteria was 1:10. The premix was then injected in a microfluidic device under pressure control to generate droplets of ~24µm of diameters, with bacteria at indicated λ , in fluorinated oil (Novec 7500 (Sigma-Aldrich), 2% EA (Raindance)). The size of the droplets is controlled by a flow-focusing step junction at the nozzle. The collected droplets were then transferred in a PCR tube, and the PCR was initiated: 95°C 3min, (98°C 10s, 53°C 30s, 72°C 1 min 30) x 35, 72°C 2 min.

Selection of KlenTaq active gene with various λ								
λ	Fraction (active/total)				Active genes (fraction) enrichment (n-fold)	SQI	Bulk final	
	initial	error	final	error			fraction	error
1st selection experiment								
0,01	5,0%		96,0%		19,2	0.96	31,7%	
0,1	7,3%		84,0%		11,5	0.86	20,7%	
1	ND*		80,0%		13,3	1.23	57,9%	
5	ND*		55,0%		9,2	2.52	24,1%	
2nd selection experiment								
0,01	20,7%	±6,9%	99,9%	±0,1%	4,8	1.00	24,63%	±10%
0,1	19,3%	±4%	97,7%	±0,7%	5,1	1.02	29,7%	±4,5%
1	16,8%	±3,5%	83,3%	±2,8%	5,0	1.29	36,6%	±11,4%
3	24,0%	±6,5%	65,9%	±9,5%	2,7	1.96	37,3%	±7%

* Values could not be determined experimentally.
We use the experimental value of 10% for SQI calculations.

Table 1: Initial and final active fraction measured by rhqPCR

Selectivity assay

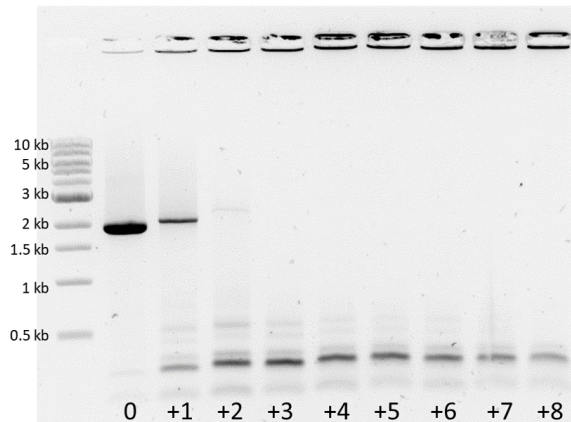
To assess the selectivity of the assay, rh qPCR reactions were run using IDT rhprimers and the RNaseH2. These primers allow to detect a single nucleotide mutation change. The rhPCR was set up using DreamTaq buffer (1x), 1.5mM of extra MgSO₄ (NEB), 200 μ M of dNTPs (NEB), 1% Evagreen (Biotium), 0.5% of DreamTaq DNA polymerase (Thermofisher) and a specific amount of RNase H2 (IDT DNA technologies), 0.3 mU for the wild-type detecting reaction and 0.2 mU for the inactive KlenTaq detection in 10 μ L reactions, and 200nM of the two adapted rhPrimers:

forward wild-type: 5'-TTGGCTGCTGGTTGCACTGGrATTATC_3SpC3

forward inactive: 5'-TTGGCTGCTGGTTGCACTGGrGTTATC_3SpC3

reverse: 5'-GCTTCACGCGGAACACCAAACrATCCAC_3SpC3

The 10 μ L reactions were monitored in CFX96 Touch Real-Time PCR Machine (Bio-rad) following a 3 min denaturation at 95°C and 40 standard qPCR cycles (95°C 10 s, 60°C 40s). Standards were run with plasmid of either active or inactive version of the gene starting from ~1 ng in 10 μ L and diluted sequentially by 5 for 5 dilutions. To determine the proper amount of RNase H2 giving the best assay dynamic range, ranges of RNase H2 were realized for each primer couple. The results were compared to control reactions performed with the corresponding classical PCR primers.



Equivalent added bacteria carrying the inactive mutant

Figure 1: Assaying the effect of droplet contamination by inactive mutants. Self-replication was run in test tubes with bacteria expressing the wild-type KlenTaq at a concentration equivalent to one bacteria per droplet (~130 bac/nL) and various amount of added bacteria expressing the mutant inactive KlenTaq (corresponding to the indicated equivalent contaminant inactive bacteria per droplet).

Estimation of the effect of the co-encapsulation of active with inactive variants

A PCR was run in Thermopol DF buffer (NEB) (1x) with 1.5mM MgSO₄, 400 µg/mL of BSA9000S (NEB), 200 µM of each dNTPs (NEB), 130 bact/nL (~1 bacteria per droplet) of bacteria expressing the active wild-type KlenTaq gene, and 200nM of reverse and forward primers:

reverse: 5'-TTAGGTCTCACTAAGCAAAAACCCCTC

forward: 5'-TTAGGTCTCATCTATAATACGACTCACTATAGGGAG.

Various amount of bacteria expressing the inactive KlenTaq mutant were added to simulate the encapsulation of the active wild-type with 1 and up to 8 inactive bacteria. PCR was run using the following protocol: 95°C 3min, (98°C 10s, 53°C 30s, 72°C 1 min 30) x 35, 72°C 2 min. Results presented on 1 show that the contamination of droplets containing one active bacteria with one inactive bacteria is greatly decreasing the reaction yield. A slight amplification is visible with 2 inactive bacteria and then no gene product is observed.

Literature review

25 articles performing high-throughput selection or screening experiment were studied and the found characteristic parameters and results are recorded in table S2 S3 and S4 according to the emulsion generation technique. All values corresponding to the initial and final quantity of the active variant were converted in ratio of active over inactive clones, when given in fraction originally.

Screening experiments with emulsion generated by shaking or filter										
#	Experiment (Target)	λ	Ratio active/inactive		Active genes enrichment (n-fold)	SQJ	Achievement In xx rounds Throughput ()			
			Initial	final						
Several λ process : gene on beads, beads in IVTT, beads in selection droplets										
1	Directed evolution of an extremely fast phosphotriesterase by In vitro compartmentalization, 2003 (Phosphotriesterase)	0.3	0.1	1.4	14	0.71	63 times higher k_{cat} In 6 rounds (6×10^6)			
			0.01	0.48	47	0.41				
			0.001	0.21	217	0.23				
2	Ribozyme-Catalyzed Transcription of an Active Ribozyme, 2011 (Ribozyme polymerase)	?	0.1	$\sim 1000^{**}$	10^4	?	Polymerase ribozyme able to synthesize a wider spectrum of RNA sequence In 13 rounds ($\sim 5 \times 10^7$)			
			0.001	$\sim 100^{**}$	10^5					
			10^{-5}	$\sim 1^{**}$	10^5					
Encapsulation of cells (bacteria or yeasts)										
3	High-Throughput Screening of Enzyme Libraries: Thiolactonases Evolved by Fluorescence-Activated Sorting of Single Cells in Emulsion Compartments, 2005 (Thiolactonase)	0.03	gating		290	0.23	100-fold improvement In activity of PON1 (paraoxonase) In 6 rounds ($\sim 5 \times 10^8$)			
			0.0001	0.001				0.29	63	0.28
			0.001	0.01				0.63	40	0.04
			0.01	0.01				0.69	69	0.42
			0.01	0.01				0	-	?
4	Ultrahigh Throughput Screening System for Directed Glucose Oxidase Evolution in Yeast Cells, 2011 (Glucose oxidase)	0.01*	*not defined		4,7	?	1,8 Increase in k_{cat} In 1 round ($\sim 10^7$)			
			0.1	0.01				13		
			0.001	0.001				33		
Encapsulation of genes by extrusion through filter										
5	High-Throughput Screening of Enzyme Libraries: In Vitro Evolution of a β -Galactosidase by Fluorescence-Activated Sorting of Double Emulsions, 2005 (β -Galactosidase)	? (300)	0.33	1	3	?	Turn a protein of unknown function into β -Galactosidase In 2 rounds (4×10^7)			
			0.008	0.82	103					
			0.008 enrich [§]	0.19	24					
			0.001	0.16	160					
<p>* not explicitly given by the authors, estimated from available data in the paper</p> <p>** estimated from gels given in the paper or sup mat by eyes</p> <p>§ enrich is an alternative mode of screening, the other most use mode in this paper is called the purify mode</p> <p>† not defined : the formula of the enrichment is not given</p> <p>‡ gating : Upper % percentile in UV fluorescence gate</p>										

Table 2: Screening experiments with emulsion generated by shaking or filter

Screening experiments with emulsion generated by microfluidic							
#	Experiment	λ	Ratio active/inactive		Active genes enrichment (n-fold)	SQI	Achievement in xx rounds Throughput ()
			initial	final			
12	High-throughput screening for industrial enzyme production hosts by droplet microfluidics, 2014 (Amylase)	?	0.25	3.5	14	?	2-fold increase in α -amylase production in 1 round (10^5)
13	A high-throughput cellulase screening system based on droplet microfluidics, 2014 (Cellulase)	?	0.001 0.014 0.078 1	0.43 1.75 7.62 21.7	430 125 97.7 21.7	?	Method development
14	Dissecting enzyme function with microfluidic-based deep mutational scanning, 2015 (β -Glucosidase)	0.1	0.54	49	90.7	1.07	Deep mutational scanning (10^7)
15	Ultra-high-throughput discovery of promiscuous enzymes by picodroplet functional metagenomics, 2015 (Detection Phosphotriesterase)	0.8	4.6×10^9	2.3×10^5	$\sim 5 \times 10^3$	4.1×10^{-4}	Identification of starting point sequences for new functions in 3 rounds (10^7 - 10^8)
16	High-throughput screening of filamentous fungi using nanoliter range droplet-based microfluidics, 2016 (α -amylase)	0.24	0.21	40.7	196	1.2	2,3 fold activity increase in 1 round (5×10^4)
17	Ultra-high-throughput-directed enzyme evolution by absorbance-activated droplet sorting (AADS), 2016 (Oxydoreductase)	1	0.0002	1.27	6350	1.12	activity >4.5-fold, kcat >2.7-fold, soluble expression 60% higher, T_m 12 °C higher in 2 rounds (10^6)
18	A general strategy for expanding polymerase function by droplet microfluidics, 2016 (Polymerase)	0.1	0.01 0.001 0.0001	70.4** 2** 0.44**	~ 4500	1.08 0.8 0.4	TNA polymerase in 1 round (3.6×10^7)

**estimated from gels given in the paper or sup mat by gel analysis with ImageJ

† not defined : the formula of the enrichment is not given

Screening experiments with emulsion generated by microfluidic							
#	Experiment	λ	Ratio active/inactive		Active genes enrichment (n-fold)	SQI	Achievement in xx rounds Throughput ()
			initial	final			
12	High-throughput screening for industrial enzyme production hosts by droplet microfluidics, 2014 (Amylase)	?	0.25	3.5	14	?	2-fold increase in α -amylase production in 1 round (10^5)
13	A high-throughput cellulase screening system based on droplet microfluidics, 2014 (Cellulase)	?	0.001	0.43	430	?	Method development
			0.014	1.75	125		
			0.078	7.62	97.7		
			1	21.7	21.7		
14	Dissecting enzyme function with microfluidic-based deep mutational scanning, 2015 (β -Glucosidase)	0.1	0.54	49	90.7	1.07	Deep mutational scanning (10^7)
15	Ultra-high-throughput discovery of promiscuous enzymes by picodroplet functional metagenomics, 2015 (Detection Phosphotriesterase)	0.8	4.6×10^{-9}	2.3×10^{-5}	$\sim 5 \times 10^3$	4.1×10^{-4}	Identification of starting point sequences for new functions in 3 rounds (10^7 - 10^8)
16	High-throughput screening of filamentous fungi using nanoliter range droplet-based microfluidics, 2016 (α -amylase)	0.24	0.21	40.7	196	1.2	2,3 fold activity increase in 1 round (5×10^4)
17	Ultra-high-throughput-directed enzyme evolution by absorbance-activated droplet sorting (AADS), 2016 (Oxydoreductase)	1	0.0002	1.27	6350	1.12	activity >4.5-fold, kcat >2.7-fold, soluble expression 60% higher, T_m 12 °C higher in 2 rounds (10^6)
18	A general strategy for expanding polymerase function by droplet microfluidics, 2016 (Polymerase)	0.1	0.01	70.4**	~ 4500	1.08	TNA polymerase in 1 round (3.6×10^7)
			0.001	2**		0.8	
			0.0001	0.44**		0.4	

**estimated from gels given in the paper or sup mat by gel analysis with ImageJ
† not defined : the formula of the enrichment is not given

Table 3: Screening experiments with emulsion generated by microfluidics

Selection experiments with emulsion generated by shaking							
#	Experiment	λ	Ratio active/inactive		Active genes enrichment (n-fold)	SQI	Achievement in xx rounds Throughput (l)
			initial	final			
Encapsulation of genes							
19	Man-made cell-like compartments for molecular evolution, 1998 (Methyltransferase)	1	0.001	1	1000	0.79	Method development (10^{10})
20	Directed Evolution of Protein Inhibitors of DNAnucleases by in Vitro Compartmentalization (IVC) and Nano-droplet Delivery, 2005 (Inhibition of self-DNA destruction)	≤ 1	0.005	0.33	66	?	claim >100 fold s 500 fold, changing protein target in 8 rounds ($\sim 10^{10}$)
			0.001	?			
			0.0004	0.05	125		
21	Selection of restriction endonucleases using artificial cells, 2007 (Restriction endonuclease)	1	0.001	>0.1	≥ 100	0.78	20-fold improvement of activity in 3 rounds (10^{10})
			0.01	1	100		
22	An in vitro Autogene, 2012 (T7 RNA polymerase mRNA)	0.01-1	0.11	4	36	?	Too many mutations arise in 4 rounds (10^6-10^{10})
Encapsulation of bacteria							
23	Directed evolution of polymerase function by compartmentalized self-replication, 2001 (Taq Polymerase)	1.7*	0.01-0.05	4.3-3.3	109	1.63	11-fold higher the mostability, 130-fold resistance to inhibitors in 3 rounds (2×10^8)
24	Directed evolution of genetic parts and circuits by compartmentalized partnered replication, 2014 (tRNA synthetase)	≤ 1 ?	0.1	2.1**	21	?	T7 RNA polymerase orthogonal promoter (40-60% WT promotor)+ unnatural amino acids incorporation by tryptophanyl tRNA-synthetase: suppressor tRNA (1500-fold) in 10 to 16 rounds ($>10^8$)
			0.01	0.6**	60		
			0.001	0.05**	50		
			0.0001	0.033**	330		
			0.00001	-			
0.05	0.27	5.4	?				
Encapsulation of complexes							
25	Compartmentalization of destabilized enzyme-mRNA-ribosome complexes generated by ribosome display: a novel tool for the directed evolution of enzymes, 2013 (Reverse Transcriptase)	0.27	0.02	1	50	0.56	3-fold activity increase, thermoresistance in 5 rounds (10^{10})
* not explicitly given by the authors, estimated from available data in the paper							
** estimated from gels given in the paper or sup mat by gel analysis with ImageJ							

Table 4: Selection experiments with emulsion generated by shaking